PHYSICAL REVIEW D **83,** 074008 (2011)

Semi-inclusive DIS cross sections and spin asymmetries in the quantum statistical parton distributions approach

Claude Bourrely*

Département de Physique, Faculté des Sciences de Luminy, Université de la Méditerranée - Aix-Marseille II, 13288 Marseille, Cedex 09, France

Franco Buccella†

Dipartimento di Scienze Fisiche, Università di Napoli, Via Cintia, I-80126, Napoli and INFN, Sezione di Napoli, Italy

Jacques Soffer‡

Department of Physics, Temple University, Philadelphia, Pennsylvania 19122-6082, USA

(Received 31 August 2010; published 11 April 2011)

We consider the extension of the statistical parton distributions to include their transverse momentum dependence, by using two different methods, one is based on our quantum statistical approach, the other on a relativistic covariant method. We take into account the effects of the Melosh-Wigner rotation for the polarized distributions. The results obtained can be compared with recent semi-inclusive deep inelastic scattering (DIS) data on the cross section and double longitudinal-spin asymmetries from JLab. We also give some predictions for future experiments on electron-neutron scattering.

DOI: 10.1103/PhysRevD.83.074008 PACS numbers: 12.40.Ee, 13.60.Hb, 13.88.+e, 14.65.Bt

I. INTRODUCTION

A new set of parton distribution functions (PDF) was constructed in the framework of a statistical approach of the nucleon [1], and let us first recall very briefly, its main characteristic features. For quarks (antiquarks), the building blocks are the helicity dependent distributions $q_{\pm}(x)$ ($\bar{q}_{\pm}(x)$) so this allows to describe simultaneously the unpolarized distributions $q(x) = q_{+}(x) + q_{-}(x)$ and the helicity distributions $\Delta q(x) = q_{+}(x) - q_{-}(x)$ (similarly for antiquarks). At the initial energy scale taken at $Q_0^2 = 4$ GeV^2, these distributions are given by the sum of two terms, a quasi Fermi-Dirac function and a helicity independent diffractive contribution, which leads to a universal behavior at very low x for all flavors. The flavor asymmetry for the light sea, i.e. $\bar{d}(x) > \bar{u}(x)$, observed in the data is built in. This is clearly understood in terms of the Pauli exclusion principle, based on the fact that the proton contains two u quarks and only one d quark. The chiral properties of QCD lead to strong relations between $q(x)$ and $\bar{q}(x)$. For example, it is found that the well established result $\Delta u(x) > 0$ implies $\Delta\bar{u}(x) > 0$ and similarly $\Delta d(x) < 0$ leads to $\Delta\bar{d}(x) < 0$. Concerning the gluon, the unpolarized distribution $G(x, Q_0^2)$ is given in terms of a quasi Bose-Einstein function, with only *one free parameter*, and for simplicity, one assumes zero gluon polarization, i.e. $\Delta G(x, Q_0^2) = 0$, at the initial energy scale Q_0^2. All unpolarized and polarized light quark distributions depend upon *eight* free parameters, which were determined in 2002 (see Ref. [1]), from a next-to-leading order fit of a selected set of accurate deep inelastic scattering (DIS) data. Concerning the strange quark and antiquark distributions, the statistical approach has been applied to calculate the strange quark asymmetry and the corresponding helicity distributions, which were found both negative at all x values [2]. More recently, new tests against experimental (unpolarized and polarized) data turned out to be very satisfactory, in particular, in hadronic reactions, as reported in Refs. [3,4]. The paper is organized as follows. In the next section we review the construction of the statistical distributions and we present an improved version of the extension to the transverse momentum dependence (TMD). In Sec. III, we will consider charged pion production in semi-inclusive deep inelastic scattering (SIDIS), $\ell N \to \ell HX$, a suitable reaction for testing our TMD distributions, more specifically, for the cross section and the longitudinal-spin asymmetry, by taking into account the effects of the Melosh-Wigner rotation. The results are given and discussed in Sec. IV and the last section is devoted to our concluding remarks.

II. THE TMD PARTON DISTRIBUTIONS

A. The original longitudinal parton distributions

We now review some of the basic features of the statistical approach, as opposed to the standard polynomial type parametrizations of the PDF, based on Regge theory at low x and counting rules at large x. The fermion distributions are given by the sum of two terms [1], a quasi Fermi-Dirac function and a helicity independent diffractive contribution equal for all light quarks:

*bourrely@cmi.univ-mrs.fr
†buccella@na.infn.it
‡jacques.soffer@gmail.com

 © 2011 American Physical Society

$$xq^h(x, Q_0^2) = \frac{AX_{0q}^h x^b}{\exp[(x - X_{0q}^h)/\bar{x}] + 1} + \frac{\tilde{A}x^{\tilde{b}}}{\exp(x/\bar{x}) + 1}, \tag{1}$$

$$x\bar{q}^h(x, Q_0^2) = \frac{\bar{A}(X_{0q}^{-h})^{-1}x^{2b}}{\exp[(x + X_{0q}^{-h})/\bar{x}] + 1} + \frac{\tilde{A}x^{\tilde{b}}}{\exp(x/\bar{x}) + 1}, \tag{2}$$

at the input energy scale $Q_0^2 = 4$ GeV^2. Notice the change of sign of the potentials and helicity for the antiquarks. The parameter $\bar{x}$ plays the role of a *universal temperature* and $X_{0q}^{\pm}$ are the two *thermodynamical potentials* of the quark q, with helicity $h = \pm$. The *eight* free parameters[1] in Eqs. (1) and (2) were determined at the input scale from the comparison with a selected set of very precise unpolarized and polarized DIS data [1]. They have the following values

$$\begin{aligned} \bar{x} &= 0.09907, & b &= 0.40962, \\ \tilde{b} &= -0.25347, & \tilde{A} &= 0.08318, \end{aligned} \tag{3}$$

$$\begin{aligned} X_{0u}^+ &= 0.46128, & X_{0u}^- &= 0.29766, \\ X_{0d}^- &= 0.30174, & X_{0d}^+ &= 0.22775. \end{aligned} \tag{4}$$

For the gluons we consider the black-body inspired expression

$$xG(x, Q_0^2) = \frac{A_G x^{b_G}}{\exp(x/\bar{x}) - 1}, \tag{5}$$

a quasi Bose-Einstein function, with $b_G = 0.90$, the only free parameter,[2] since $A_G = 20.53$ is determined by the momentum sum rule. We also assume that, at the input energy scale, the polarized gluon, distribution vanishes, so

$$x\Delta G(x, Q_0^2) = 0. \tag{6}$$

For the strange quark distributions, the simple choice made in Ref. [1] was greatly improved in Ref. [2], but they will not be considered in this paper. In Eqs. (1) and (2) the multiplicative factors X_{0q}^h and $(X_{0q}^{-h})^{-1}$ in the numerators of the nondiffractive parts of q's and $\bar{q}$'s distributions imply a modification of the quantum statistical form we were led to propose in order to agree with experimental data. The presence of these multiplicative factors was justified in our earlier attempt to generate the TMD [5], as we will explain now, with a considerable improvement.

[1] $A = 1.74938$ and $\bar{A} = 1.90801$ are fixed by the following normalization conditions $u - \bar{u} = 2$, $d - \bar{d} = 1$.

[2] In Ref. [1] we were assuming that, for very small x, $xG(x, Q_0^2)$ has the same behavior as $x\bar{q}(x, Q_0^2)$, so we took $b_G = 1 + \tilde{b}$. However this choice leads to a too much rapid rise of the gluon distribution, compared to its recent determination from Hadron Elektron Ring Anlage (HERA) data, which requires $b_G = 0.90$.

B. The TMD statistical distributions revisited

Let us recall that the TMD of the nondiffractive part of a quark distribution q of helicity h (first term in Eq. (1)) was introduced by the following multiplicative term

$$\frac{1}{\exp[(k_T^2/x\mu^2 - Y_{0q}^h)/\bar{x}] + 1}, \tag{7}$$

where Y_{0q}^h is the thermodynamical potential associated to the quark transverse momentum k_T and $1/\mu^2$ is a Lagrange multiplier, whose value is determined by a transverse energy sum rule. We notice that this term induces a non factorizable x and k_T dependence as it is assumed in some other parametrizations. In order to recover the original x distributions, the integration of (7) over k_T^2 gives the explicit factor

$$\begin{aligned} &\int_0^\infty \frac{dk_T^2}{\exp[(k_T^2/x\mu^2 - Y_{0q}^h)/\bar{x}] + 1} \\ &\quad = -x\mu^2\bar{x}\mathrm{Li}_1(-\exp[Y_{0q}^h/\bar{x}]). \end{aligned} \tag{8}$$

Here Li_1 denotes the polylogarithm function of order 1, which is known to arise from the integral of Fermi-Dirac distributions and is such that

$$-\mathrm{Li}_1(-e^y) = \int_0^\infty \frac{d\omega}{e^{(\omega - y)} + 1} = \ln(1 + e^y). \tag{9}$$

Similarly for an antiquark distribution $\bar{q}$ of helicity $-h$, according to the rules of the statistical approach, one should use the same potential with the opposite sign, so one gets instead, $x\mu^2\bar{x}\ln(1 + \exp[-Y_{0q}^h/\bar{x}])$. In Ref. [5], we made the arbitrary simple choice $Y_{0q}^h = kX_{0q}^h$, with $k = 1.42$, which allows to recover the factor X_{0q}^h for quarks (see Eq. (1)), since for large values [3] of $Y_{0q}^h/\bar{x}$, one has $\mathrm{Li}_1(-\exp[Y_{0q}^h/\bar{x}]) \sim Y_{0q}^h/\bar{x}$, which is proportional to X_{0q}^h. However this is not suitable to get the factor $[X_{0q}^h]^{-1}$ for antiquarks (see Eq. (2)), because $\mathrm{Li}_1(-\exp[-Y_{0q}^h/\bar{x}]) \sim \exp[-Y_{0q}^h/\bar{x}]$ for large values of $Y_{0q}^h/\bar{x}$. In other words, the product $\ln(1 + \exp[Y_{0q}^h/\bar{x}]) \cdot \ln(1 + \exp[-Y_{0q}^h/\bar{x}])$ does not remain independent of Y_{0q}^h, as it should. Actually, the division by $\bar{x}$ of the argument of the exponential in the Fermi-Dirac expression was not necessary because for the transverse degrees of freedom, μ^2 plays the role of the temperature. This feature reflects the fact that one should not treat on equal footing longitudinal and transverse degrees of freedom. Therefore, for the sake of simplicity, we propose to replace Eq. (7) by

$$\frac{1}{\exp(k_T^2/x\mu^2 - Y_{0q}^h) + 1}, \tag{10}$$

[3] $\bar{x}$ has a small value according to Eq. (3) above.

with the corresponding integral over k_T^2, $x\mu^2 \ln(1+\exp[Y_{0q}^h])$. Clearly this implies a different normalization for μ^2 and Y_{0q}^h. At high k_T, Eq. (10) has a Gaussian behavior, with a width proportional to $\mu\sqrt{x}$, at variance with the usual factorization assumption of the dependences in x and k_T [6]. The product $\ln(1+\exp[Y_{0q}^h]) \cdot \ln(1+\exp[-Y_{0q}^h])$ has its maximum $(\ln 2)^2$ for $Y_{0q}^h = 0$ and therefore it is stationary around this value. So now in order to try to recover the factors X_{0q}^h and $(X_{0q}^{-h})^{-1}$ in Eqs. (1) and (2), we simply have to choose Y_{0q}^h such that $\ln(1+\exp[Y_{0q}^h])$ is proportional to X_{0q}^h and more precisely such that

$$\ln(1+\exp[Y_{0q}^h]) = kX_{0q}^h. \tag{11}$$

This way we recover exactly the factors X_{0q}^h introduced in Eq. (1) for the quarks. We take the proportionality factor $k = \ln 2/X_{0d}^+$, X_{0d}^+ being the lowest longitudinal potential, so with the value given in (4) we get $k = 3.05$. In order to get almost exactly $(X_{0q}^h)^{-1}$ for the antiquarks in Eq. (2), we also assume that the corresponding transverse potential Y_{0d}^+ is small and fixed to the value 0.01. So from Eq. (11), the values of the other three transverse potentials can be obtained and we finally have

$$\begin{aligned} Y_{0u}^+ &= 1.122, \qquad Y_{0u}^- = 0.388, \\ Y_{0d}^- &= 0.409, \qquad Y_{0d}^+ = 0.010. \end{aligned} \tag{12}$$

These are different from the values obtained in Ref. [5] and will lead to different predictions for the TMD of the PDF. The nondiffractive contributions read now

$$xq^h(x,k_T^2) = \frac{F(x)}{\exp(x - X_{0q}^h)/\bar{x} + 1} \times \frac{1}{\exp(k_T^2/x\mu^2 - Y_{0q}^h) + 1}, \tag{13}$$

$$x\bar{q}^h(x,k_T^2) = \frac{\bar{F}(x)}{\exp(x + X_{0q}^{-h})/\bar{x} + 1} \times \frac{1}{\exp(k_T^2/x\mu^2 + Y_{0q}^{-h}) + 1}, \tag{14}$$

where

$$F(x) = \frac{Ax^{b-1}X_{0q}^h}{\ln(1+\exp Y_{0q}^h)\mu^2} = \frac{Ax^{b-1}}{k\mu^2}. \tag{15}$$

Similarly for $\bar{q}$ we have $\bar{F}(x) = \bar{A}x^{2b-1}/k\mu^2$. After this new determination of the transverse potentials, we will see later how we can determine μ^2, using the transverse energy sum rule. As noted in Ref. [5], if p_z denotes the proton momentum, its energy can be approximated by $p_z + M^2/2p_z$, where M is the proton mass. Similarly the energy of a massless parton, with transverse momentum k_T is, in the same approximation, $xp_z + k_T^2/2xp_z$. Therefore all involved parton distributions denoted $p_i(x,k_T^2)$ must satisfy the momentum sum rule

$$\sum_i \int_0^1 dx \int x p_i(x,k_T^2) dk_T^2 = 1, \tag{16}$$

and also the transverse energy sum rule

$$\sum_i \int_0^1 dx \int p_i(x,k_T^2) \frac{k_T^2}{x} dk_T^2 = M^2. \tag{17}$$

The contribution of Eq. (13), for the quarks, to the sum rule Eq. (17) is given by:

$$\int \frac{k_T^2}{x} q^h(x,k_T^2) dx dk_T^2 = \int_0^1 \frac{F(x)dx}{x^2\left(\exp\frac{x - X_{0q}^h}{\bar{x}} + 1\right)} \times \int_0^\infty \frac{k_T^2 dk_T^2}{\exp\left(\frac{k_T^2}{x\mu^2} - Y_{0q}^h\right) + 1}, \tag{18}$$

and after the change of variable $\xi = k_T^2/x\mu^2$, we get

$$\mu^2 \int_0^1 \frac{\mu^2 F(x)dx}{\exp\frac{x - X_{0q}^h}{\bar{x}} + 1} \int_0^\infty \frac{\xi d\xi}{\exp(\xi - Y_{0q}^h) + 1} = \mu^2 I_1 \cdot I_2, \tag{19}$$

where

$$I_1 = \int_0^1 \frac{\mu^2 F(x)dx}{\exp\frac{x - X_{0q}^h}{\bar{x}} + 1} = \frac{P_{q^h}}{\ln(1+\exp Y_{0q}^h)}, \tag{20}$$

P_{q^h} is the number of parton of type q^h, and

$$I_2 = \int_0^\infty \frac{\xi d\xi}{\exp(\xi - Y_{0q}^h) + 1} = \frac{\pi^2}{6} + \frac{(Y_{0q}^h)^2}{2} + \mathrm{Li}_2(-\exp(-Y_{0q}^h)). \tag{21}$$

Therefore in the limit $Y_{0q}^h = 0$ the contribution of a parton of type q^h is just $\mu^2 P_{q^h}\pi^2/(12\ln 2)$, since $\mathrm{Li}_2(-1) = -\pi^2/12$.

In a similar way for the contribution to the sum rule Eq. (17), from the nondiffractive part of the light antiquarks Eq. (14), we get

$$\mu^2 \int_0^1 \frac{\mu^2 \bar{F}(x)dx}{\exp\frac{x + X_{0q}^{-h}}{\bar{x}} + 1} \int_0^\infty \frac{\xi d\xi}{\exp(\xi + Y_{0q}^{-h}) + 1} = \mu^2 \bar{I}_1 \cdot \bar{I}_2, \tag{22}$$

where

$$\bar{I}_1 = \int_0^1 \frac{\mu^2 \bar{F}(x)dx}{\exp\frac{x+X_{0q}^{-h}}{\bar{x}} + 1} = \frac{P_{\bar{q}^h}}{\ln(1+\exp(-Y_{0q}^{-h}))}, \quad (23)$$

$P_{\bar{q}^h}$ is the number of parton of type $\bar{q}^h$, and

$$\bar{I}_2 = \int_0^\infty \frac{\xi d\xi}{\exp(\xi + Y_{0q}^{-h}) + 1} = \frac{\pi^2}{6} + \frac{(Y_{0q}^{-h})^2}{2} + \mathrm{Li}_2(-\exp(Y_{0q}^{-h})). \quad (24)$$

Finally we turn to the universal diffractive contribution to quarks and antiquarks in Eqs. (1) and (2), namely $xq^D(x, Q_0^2) = \tilde{A}x^{\tilde{b}}/[\exp(x/\bar{x}) + 1]$. Since $\tilde{b} < 0$ (see Eq. (3)), the introduction of the k_T dependence cannot be done similarly to the nondiffractive contributions, because in the energy sum rule Eq. (17), it generates a singular behavior when $x \to 0$. Therefore in order to avoid this difficulty, as in Ref. [5], we modify our prescription by taking at the input energy scale

$$xq^D(x, k_T^2) = \frac{\tilde{A}x^{\tilde{b}-2}}{\ln 2\mu^2} \frac{1}{[\exp(x/\bar{x}) + 1]} \frac{1}{[\exp(k_T^2/x^2\mu^2) + 1]}, \quad (25)$$

whose k_T fall off is stronger, because $x\mu^2$ is now replaced by $x^2\mu^2$. Note that this is properly normalized to recover $xq^D(x, Q_0^2)$ after integration over k_T^2. We have checked that $xq^D(x, k_T^2)$ gives a negligible contribution to Eq. (17), as expected (See Appendix). Concerning the gluon, since it is parametrized by a quasi Bose-Einstein function, one has to introduce a nonzero potential Y_G, in contrast with the QCD equilibrium conditions, to avoid the singular behavior of $\mathrm{Li}_1(\exp[-Y_G/\bar{x}])$, when $Y_G = 0$. The value of Y_G is not constrained, but by taking a very small Y_G, it does not affect the energy sum rule (See Appendix). Clearly these regularization procedures to the diffractive contribution and to the gluon are not fully satisfactory, but we will discuss them again in our concluding remarks (See Sec. V). By summing up all contributions to the energy sum rule, one finally gets the value of μ^2, namely $\mu^2 = 0.198\ \mathrm{GeV}^2$.

C. The Melosh-Wigner transformation

So far in all our quark or antiquark TMD distributions (see Eqs. (13) and (14)), the label "'h'" stands for the helicity along the longitudinal momentum and not along the direction of the momentum, as normally defined for a genuine helicity. The basic effect of a transverse momentum $k_T \neq 0$ is the Melosh-Wigner rotation [7,8], which mixes the components $q^\pm$ in the following way

$$q^{+'} = \cos^2\theta q^+ + \sin^2\theta q^- \quad \text{and}$$
$$q^{-'} = \cos^2\theta q^- + \sin^2\theta q^+, \quad (26)$$

where $2\theta = \mathrm{Arctg}(\kappa k_T/xM)$, M is the proton mass and κ is a dimensionless parameter. Consequently $q = q^+ + q^-$ remains unchanged $q' = q$, whereas we have

$$\Delta q' = (\cos^2\theta - \sin^2\theta)\Delta q = \cos 2\theta \Delta q = \cos \mathrm{Arctg}(\kappa k_T/xM)\Delta q. \quad (27)$$

So we finally get

$$\Delta q' = \frac{1}{\sqrt{1 + (\kappa k_T/xM)^2}} \Delta q. \quad (28)$$

The effect of the Melosh-Wigner transformation on the double longitudinal-spin asymmetry will be discussed in Sec. IV.

D. The TMD distributions in the relativistic covariant approach

Covariant parton models have been widely discussed in the literature, but in some recent papers [9,10], an analysis based on the requirements of symmetry, for the parton motion in the nucleon rest frame, leads to a different method to generate the TMD of a given x-distribution. By using some input unpolarized distribution $f(x)$, one can calculate the corresponding TMD distribution $f(x, k_T^2)$, by means of its derivative, according to the following rule

$$f(x, k_T^2) = -\frac{1}{\pi M^2} \frac{d}{d\xi}(f(\xi)/\xi), \quad (29)$$

where the variable ξ is defined as $\xi = x(1 + k_T^2/x^2M^2)$, M being the proton mass. This method has been generalized for helicity distributions $\Delta f(x)$ and in this case we have for the corresponding TMD distribution $\Delta f(x, k_T^2)$

$$\Delta f(x, k_T^2) = \frac{2x - \xi}{\pi M^2 \xi^3} \times \left[3\Delta f(\xi) + 2\int_\xi^1 \frac{\Delta f(y)}{y} dy - \xi \frac{d}{d\xi}\Delta f(\xi)\right]. \quad (30)$$

It is interesting to recall that in Ref. [11], it was demonstrated that for the TMD PDF a factorized form $f_1(x)f_2(k_T^2)$ is in contradiction with the Lorentz structure, at least for a zero strong interaction coupling $g = 0$. Using a rather different approach, they obtain results identical to the ones above. We will show and discuss later the results one obtains from these formulas, using as input the x-dependent statistical PDF in Eqs. (1) and (2). In this approach as well as in ours, one gets the distributions function of x and k_T^2/x.

III. CROSS SECTION AND SPIN ASYMMETRY OF PION PRODUCTION IN POLARIZED SIDIS

Following Ref. [12], we consider the polarized SIDIS, $\ell N \to \ell H X$ in the simple quark-parton model, with unintegrated parton distributions. According to the standard notations for DIS variables, ℓ and ℓ' are, respectively, the four-momenta of the initial and the final state leptons, $q = \ell - \ell'$ is the exchanged virtual photon momentum, P is the target nucleon momentum, P_H is the final hadron momentum, $Q^2 = -q^2$, $x = Q^2/2P\cdot q$, $y = P\cdot q/P\cdot \ell$, $z = P\cdot P_H/P\cdot q$, $Q^2 = xy(s - M^2)$ and $s = (\ell + P)^2$. We work in a frame with the z-axis along the virtual photon momentum direction and the x-axis in the lepton scattering plane, with positive direction chosen along the lepton transverse momentum. The produced hadron has transverse momentum p_T (For further details see Ref. [12]). Keeping only twist-two contributions and terms up to $\mathcal{O}(M/Q)$, the cross section for SIDIS of longitudinally polarized leptons off a longitudinally polarized target can be written as:

$$\frac{d^5\sigma^{\overrightarrow{\Leftarrow}}}{dxdydzd^2p_T} = \frac{2\alpha^2}{xy^2s}\{\mathcal{H}_1 + \lambda S_L \mathcal{H}_2\}, \tag{31}$$

where the arrows indicate the direction of the lepton ($\rightarrow$) and target nucleon ($\Leftarrow$) polarizations, with respect to the lepton momentum; λ, and S_L are the magnitudes of the longitudinal beam polarization and the longitudinal target polarization, respectively.

The two terms have the following simple partonic expressions

$$\mathcal{H}_1(p_T) = \sum_q e_q^2 \int d^2k_T q(x,k_T)\pi y^2 \frac{\hat{s}^2+\hat{u}^2}{Q^4} D_q^h(z,q_T), \tag{32}$$

$$\mathcal{H}_2(p_T) = \sum_q e_q^2 \int d^2k_T \Delta q'(x,k_T)\pi y^2 \frac{\hat{s}^2-\hat{u}^2}{Q^4} D_q^h(z,q_T), \tag{33}$$

where $p_T = q_T + zk_T$ and q_T is the intrinsic transverse momentum of the hadron H with respect to the fragmenting quark direction. Here $\hat{s}$, $\hat{t}$ and $\hat{u}$ are the Mandelstam variables for the subprocess $\ell q \to \ell q$. Note that in Eq. (33) above, we have used Eq. (28), which takes into account the effect of the Melosh-Wigner rotation. The first two contributions, Eqs. (32) and (33), give, respectively, the unpolarized cross section and the numerator of the double longitudinal-spin asymmetry A_1

$$\begin{aligned}\frac{d^5\sigma^{++}}{dxdydzd^2p_T} - \frac{d^5\sigma^{+-}}{dxdydzd^2p_T} &= \frac{4\alpha^2}{xy^2s}\mathcal{H}_2,\\ \frac{d^5\sigma}{dxdydzd^2p_T} &= \frac{2\alpha^2}{xy^2s}\mathcal{H}_1,\end{aligned} \tag{34}$$

where $+$, $-$ stand for helicity states. So we simply have $A_1 = 2\mathcal{H}_2/\mathcal{H}_1$.

The integrals in Eqs. (32) and (33) involve the following TMD fragmentation function [13]

$$D_q^h(z,q_T) = D_q^h(z)\frac{1}{\pi\mu_D^2}\exp\left(-\frac{q_T^2}{\mu_D^2}\right), \tag{35}$$

which is the standard factorized Gaussian model, since we have not yet generalized our statistical approach to the TMD fragmentation functions.

IV. RESULTS AND DISCUSSION

In this section we will present all our results on the TMD unpolarized and polarized PDF, for light quarks and antiquarks, resulting from the two approaches considered above. We will discuss their specific features and the difference they lead to, in the calculation of the cross sections and the spin asymmetries for SIDIS pion production. All our results are given at $Q^2 = 2.37$ GeV^2, the value corresponding to the CLAS data [14,15], so we have performed a backward QCD evolution from our input energy scale $Q_0^2 = 4$ GeV^2. In Fig. 1 we show $xu(x,k_T,Q^2)$ and $xd(x,k_T,Q^2)$ as a function of k_T for different x values, using the TMD statistical PDF constructed in Sec. II B. We have checked that in this x-region, the nondiffractive part of the quark distributions largely dominate. Similarly $x\Delta u(x,k_T,Q^2)$ and $x\Delta d(x,k_T,Q^2)$ are shown in Fig. 2 and we recall that they are independent of the diffractive contribution. It is clear that all these k_T distributions are close to a Gaussian behavior, but with a x-dependent width. The corresponding antiquark PDF are shown in Figs. 3 and 4 and in this case, we notice a much more rapid fall off in k_T compare to the unpolarized PDF. Now if one uses the procedure resulting from the relativistic covariant approach described in Sec. II D, one obtains different TMD unpolarized and polarized PDF as shown in Figs. 5 and 6 for u and d quarks. By comparing them with Figs. 1 and 2, we see that their k_T fall off is much faster than in the previous case. The corresponding antiquark distributions are shown in Figs. 7 and 8. Next, we turn to the calculation of the unpolarized cross section and the double longitudinal-spin asymmetry for pion production in polarized SIDIS. The cross section is directly related to $\mathcal{H}_1$ (see Eq. (34)) and we show in Fig. 9, the results, on a proton target, from the two approaches, versus p_T^2, for different x-values. The parameter μ_D^2, which enters in the fragmentation function, Eq. (35), is a free parameter. In order to get the best description of the data of Ref. [14], it has been adjusted

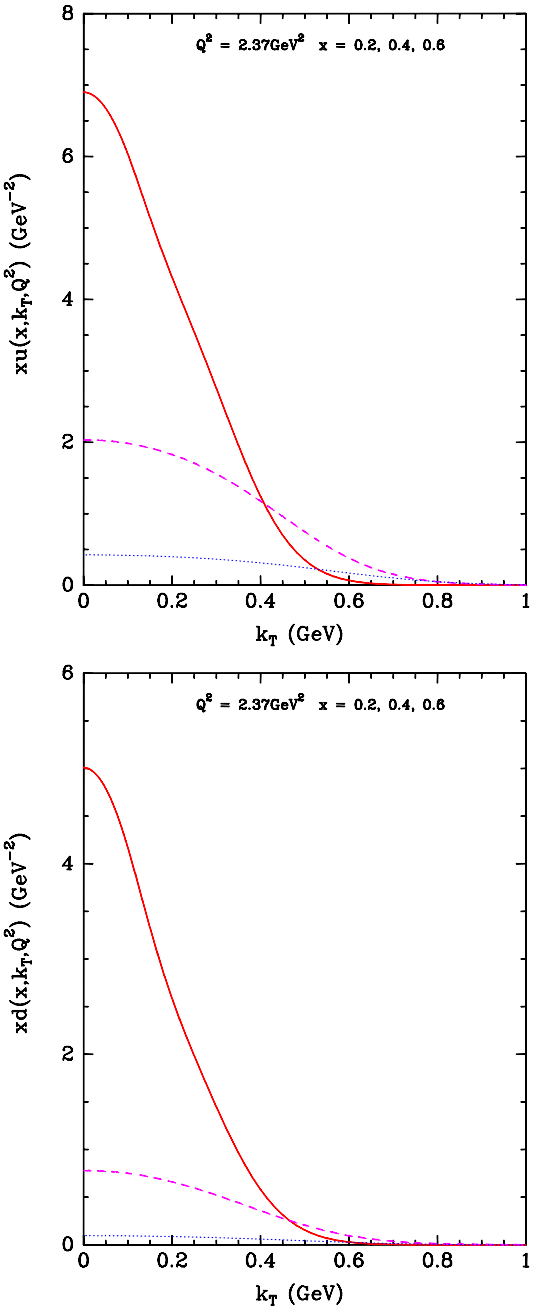

FIG. 1 (color online). The statistical distributions $xu(x, k_T, Q^2)$ (*top*) and $xd(x, k_T, Q^2)$ (*bottom*), calculated at $Q^2 = 2.37$ GeV^2, versus k_T, for different x values: solid line $x = 0.2$, dashed line $x = 0.4$, dotted line $x = 0.6$.

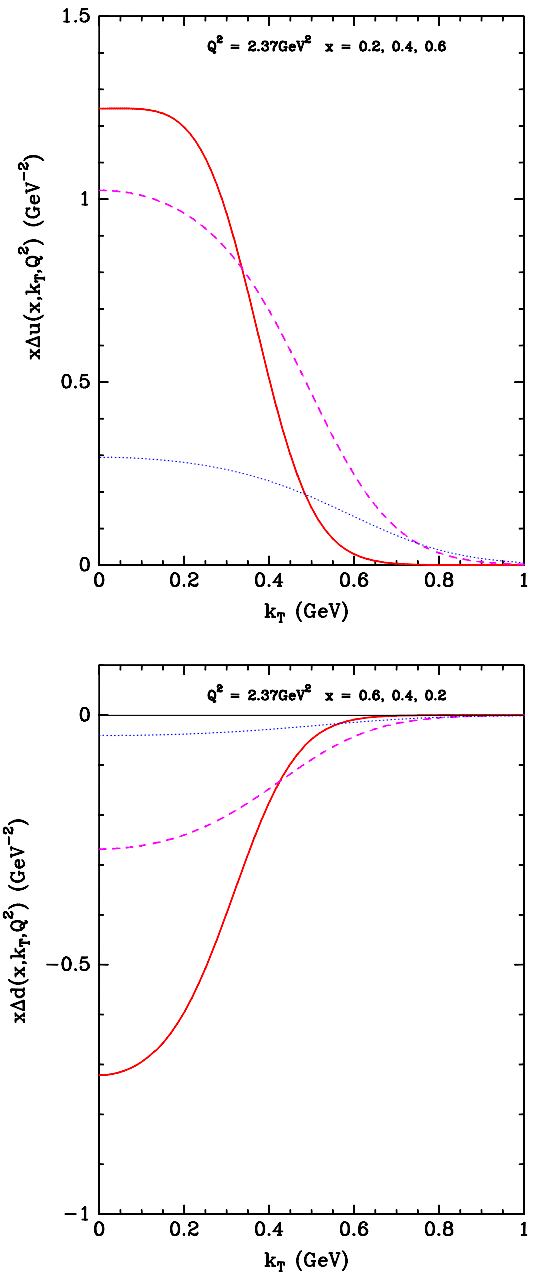

FIG. 2 (color online). The statistical distributions $x\Delta u(x, k_T, Q^2)$ (*top*) and $x\Delta d(x, k_T, Q^2)$ (*bottom*), calculated at $Q^2 = 2.37$ GeV^2, versus k_T, for different x values: solid line $x = 0.2$, dashed line $x = 0.4$, dotted line $x = 0.6$.

to the value $\mu_D^2 = 0.155$ GeV^2, a value slightly different from the one used in Ref. [6]. The agreement is better in the case of the relativistic covariant approach, which has a faster p_T^2 fall off. However it has very little x-dependence, which is not known experimentally at the moment, unfortunately. We predict essentially the same result for π^- production and also for $\pi^\pm$ production on a neutron target.

However if we consider the ratio of the cross sections for the production of a π^+ from a neutron target over its production from a proton target, our prediction is shown in Fig. 10. The calculation was done in the two approaches considered and the results are almost identical. At fixed p_T, this ratio decreases with x, following almost the trend of the ratio $d(x)/u(x)$ (see Fig. 4 of Ref. [4]) and at fixed x, it is essentially flat over p_T, because the TMD of the pion fragmentation function is flavor independent. This prediction is worthwhile to check with future experiments.

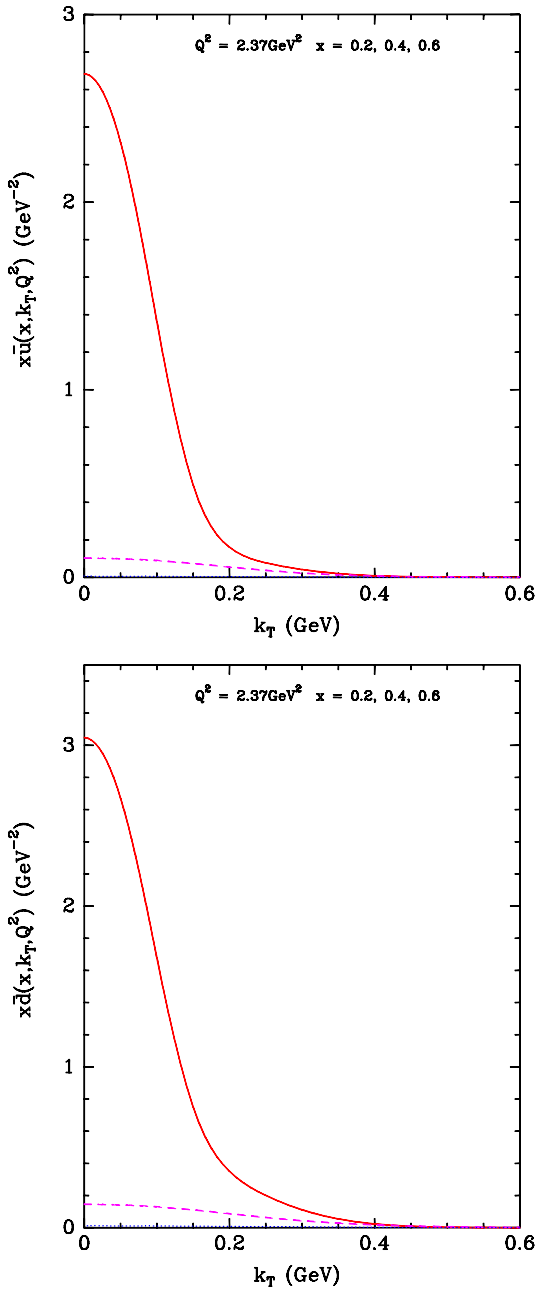

FIG. 3 (color online). The statistical distributions $x\bar{u}(x, k_T, Q^2)$ (*top*) and $x\bar{d}(x, k_T, Q^2)$ (*bottom*), calculated at $Q^2 = 2.37$ GeV^2, versus k_T, for different x values: solid line $x = 0.2$, dashed line $x = 0.4$, dotted line $x = 0.6$.

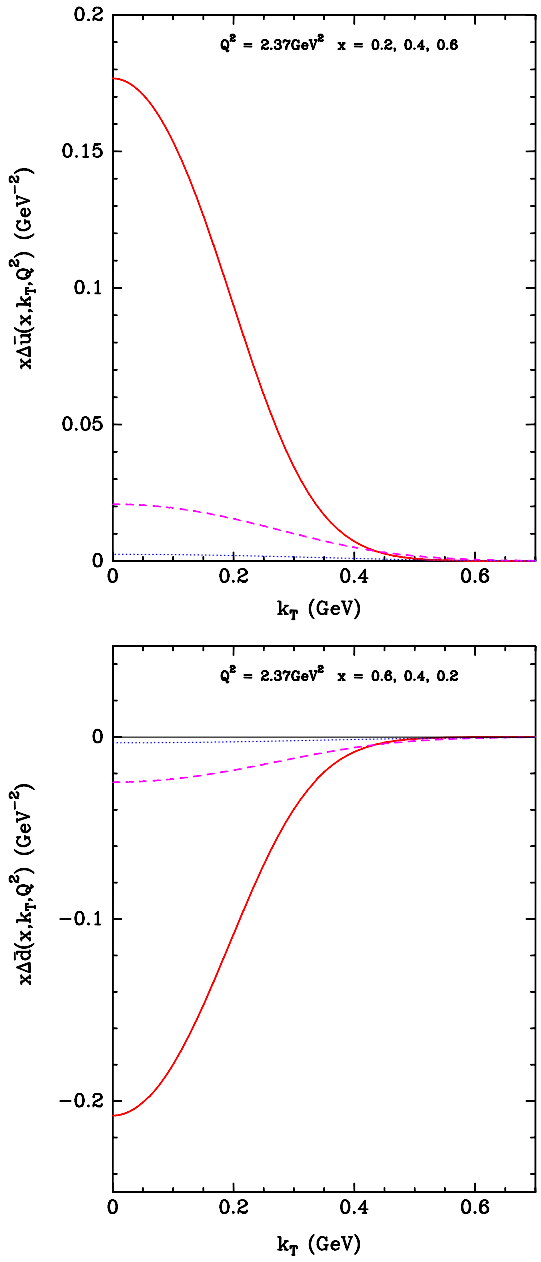

FIG. 4 (color online). The statistical distributions $x\Delta\bar{u}(x, k_T, Q^2)$ (*top*) and $x\Delta\bar{d}(x, k_T, Q^2)$ (*bottom*), calculated at $Q^2 = 2.37$ GeV^2, versus k_T, for different x values: solid line $x = 0.2$, dashed line $x = 0.4$, dotted line $x = 0.6$.

Finally, let us consider the double longitudinal-spin asymmetry A_1, defined above. The results of the calculation from both approaches, for $\pi^{\pm,0}$ on a proton target are shown in Fig. 11, with the kinematic cuts corresponding to the JLab recent data [15]. Whereas the relativistic covariant approach leads to an asymmetry decreasing with p_T, the statistical approach leads to a flat dependence in p_T, in fairly good agreement with the data, and it gives the correct normalization. We note that this behavior, which was obtained with $\kappa = 1.35$ in (28), is partly due to the effect of the Melosh-Wigner rotation. In both approaches this effect reduces A_1, but it plays an essential role in the statistical approach because it compensates the effect of the k_T rising behavior of Δq. For completeness, in view of future experiments, we have also calculated the asymmetry on a neutron target, which are displayed in Fig. 12. For the production of π^+, A_1 is sensitive to Δd and this is the reason for a negative result. In this case, the predictions from the two approaches lead again to rather different

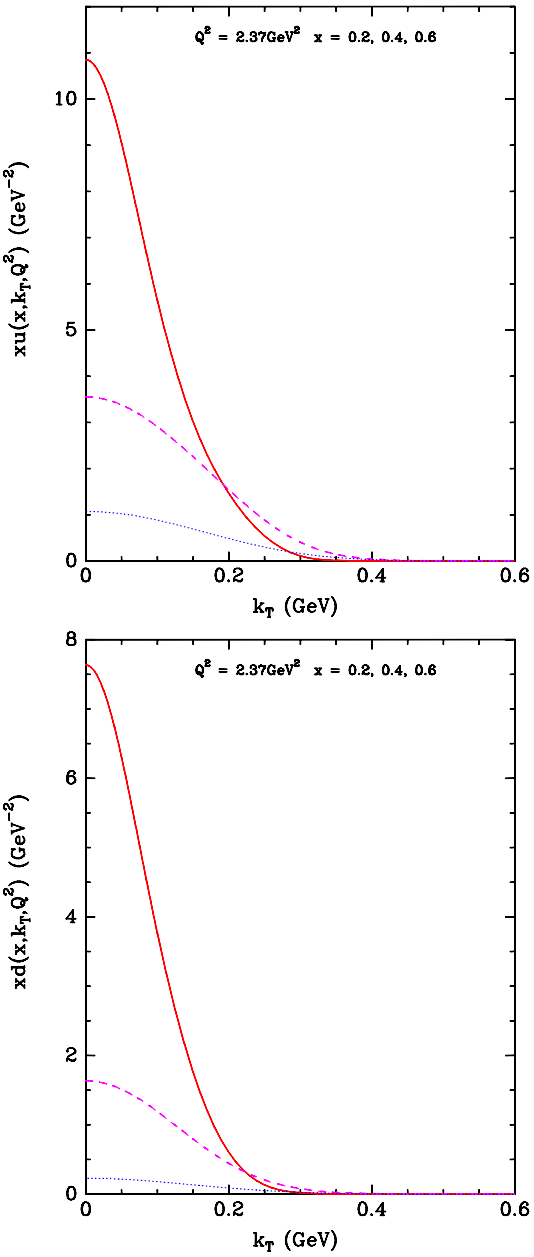

FIG. 5 (color online). The relativistic covariant distributions $xu(x, k_T, Q^2)$ (*top*) and $xd(x, k_T, Q^2)$ (*bottom*), calculated at $Q^2 = 2.37$ GeV^2, versus k_T, for different x values: solid line $x = 0.2$, dashed line $x = 0.4$, dotted line $x = 0.6$.

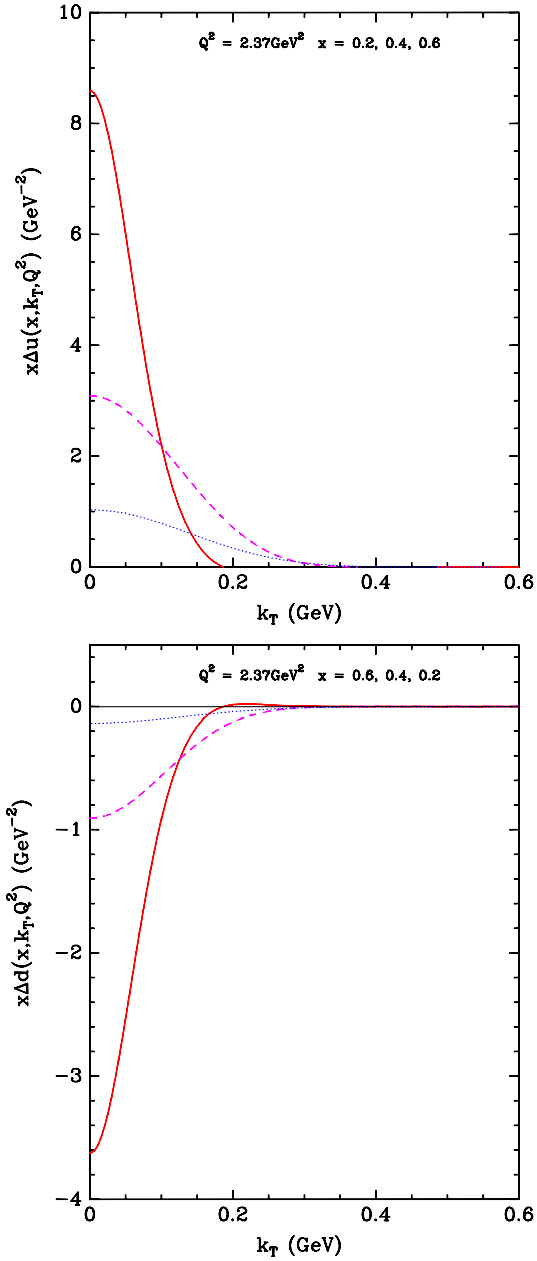

FIG. 6 (color online). The relativistic covariant distributions $x\Delta u(x, k_T, Q^2)$ (*top*) and $x\Delta d(x, k_T, Q^2)$ (*bottom*), calculated at $Q^2 = 2.37$ GeV^2, versus k_T, for different x values: solid line $x = 0.2$, dashed line $x = 0.4$, dotted line $x = 0.6$.

results, which should be also compared to the predictions from Ref. [6].

Before closing this discussion we must come back to the effect of the Melosh-Wigner rotation. It is clear that the integral over k_T of $\Delta q'$ (see Eq. (28) is smaller than $\Delta q(x)$. Therefore to solve this small mismatch, one should adjust the potentials, in such a way that $X^+_{0q} - X^-_{0q}$ increases slightly, whereas $X^+_{0q} + X^-_{0q}$ remains unchanged, since the Melosh-Wigner rotation does not affect the unpolarized distribution q. This new improvement will be considered more seriously in future work, when we will have access to more precise data on the k_T dependence of the quark distributions, allowing also a good flavor separation between u and d quarks.

V. CONCLUDING REMARKS

An important result of this work is the construction of a new set of TMD statistical distributions. This allows us to take into account, in a satisfactory way, the multiplicative

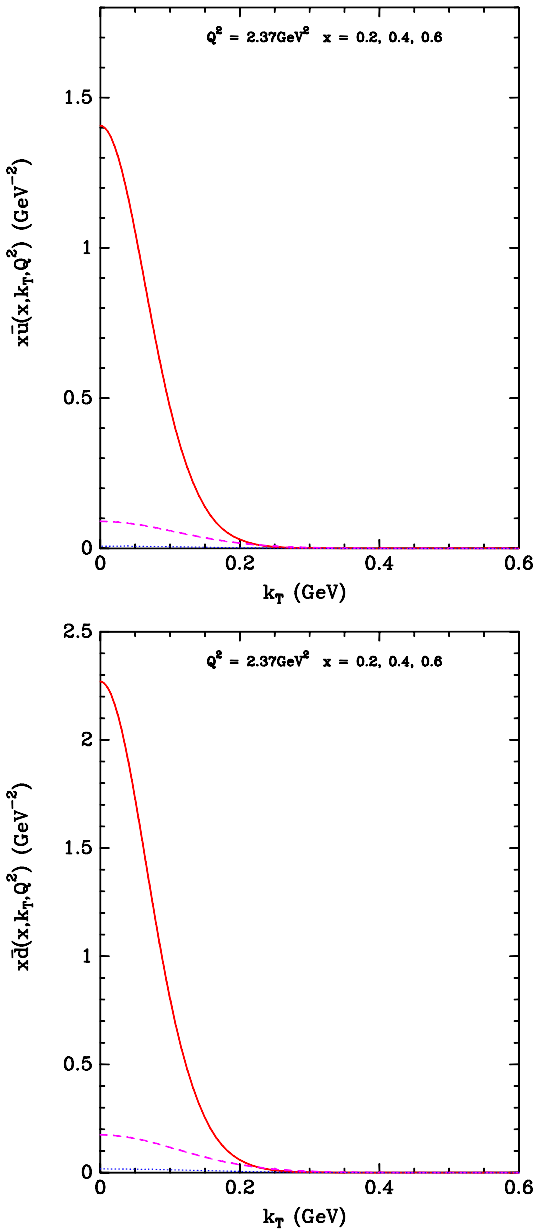

FIG. 7 (color online). The relativistic covariant distributions $x\bar{u}(x, k_T, Q^2)$ (*top*) and $x\bar{d}(x, k_T, Q^2)$ (*bottom*), calculated at $Q^2 = 2.37$ GeV^2, versus k_T, for different x values: solid line $x = 0.2$, dashed line $x = 0.4$, dotted line $x = 0.6$.

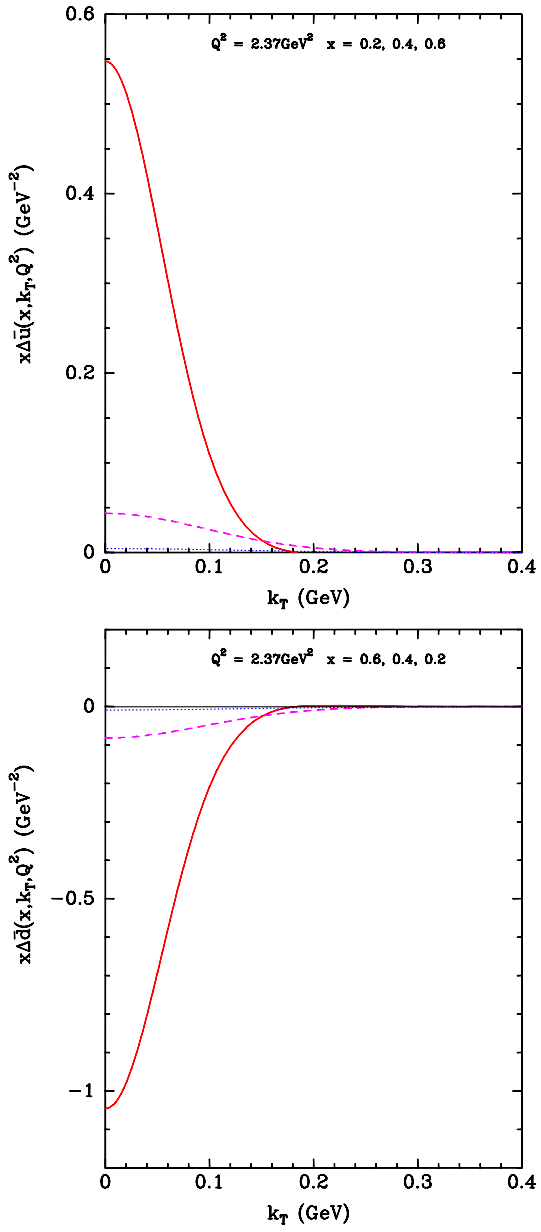

FIG. 8 (color online). The relativistic covariant distributions $x\Delta\bar{u}(x, k_T, Q^2)$ (*top*) and $x\Delta\bar{d}(x, k_T, Q^2)$ (*bottom*), calculated at $Q^2 = 2.37$ GeV^2, versus k_T, for different x values: solid line $x = 0.2$, dashed line $x = 0.4$, dotted line $x = 0.6$.

factors X_{0q}^h and $(X_{0q}^{-h})^{-1}$ in the numerators of the nondiffractive parts of q's and $\bar{q}$'s distributions. We have introduced some thermodynamical potentials Y_{0q}^h, associated to the quark transverse momentum k_T, and related to X_{0q}^h by the simple relation $\ln(1 + \exp[Y_{0q}^h]) = kX_{0q}^h$. This approach involves a parameter μ^2, which plays the role of the temperature for the transverse degrees of freedom and whose value was determined by the transverse energy sum rule. The substitution $x \to x^2$, we had to make in the diffractive part of the quark (antiquark) distributions and in the gluon distribution,[4] to avoid a singularity in the energy sum rule, remains an open problem at the moment.

We can give the intuitive argument that gluons, as photons in a laser, are created mainly in the forward direction. The diffractive part, which comes from their conversion into $q\bar{q}$ pairs, as well as the gluons themselves, may thermalize only for the x degree of freedom. We have

[4]Let us recall that, unlike the nondiffractive part, they did not require any multiplicative factor.

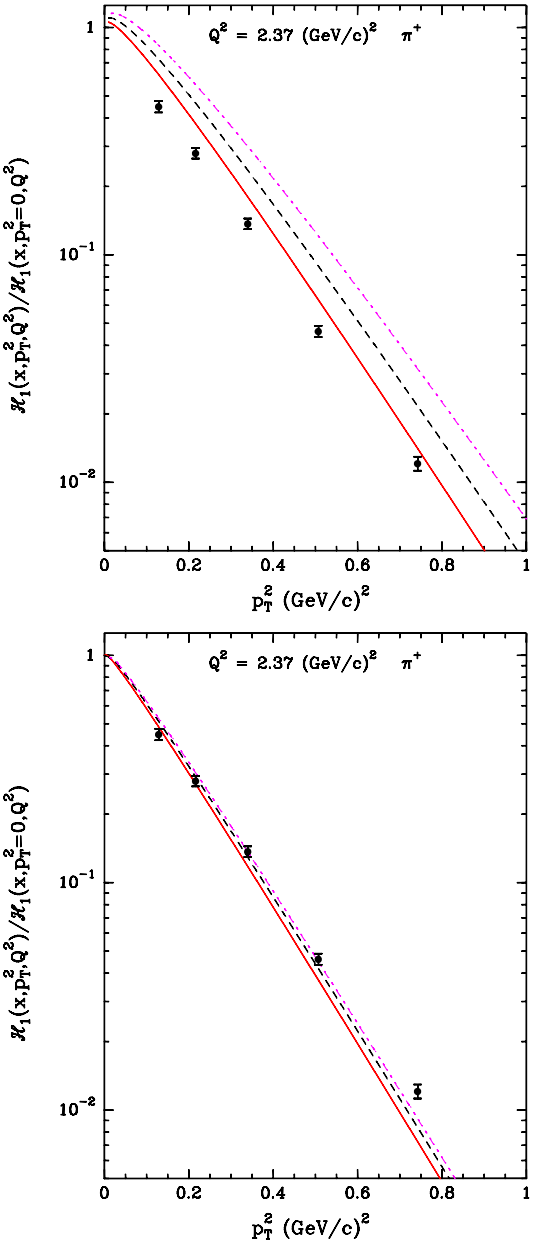

FIG. 9 (color online). The p_T^2 dependence of the term $\mathcal{H}_1$ at $Q^2 = 2.37$ GeV^2 and $z = 0.30$ for π^+ production on a proton target. Comparison of the results of the statistical approach (*top*) and the relativistic covariant distributions (*bottom*). In both cases the solid lines are for $x = 0.20$, the dashed lines for $x = 0.40$ and the dotted lines for $x = 0.60$. The data are from Ref. [14] for $x = 0.24$ and the error bars are statistical only.

calculated the p_T dependence of SIDIS cross sections and double longitudinal-spin asymmetries, taking into account the effects of the Melosh-Wigner rotation, for $\pi^{\pm,0}$ production by using this set of TMD parton distributions and another set coming from the relativistic covariant approach. These sets lead to different results, which were compared to recent experimental data. Both sets do not satisfy the usual factorization assumption of the

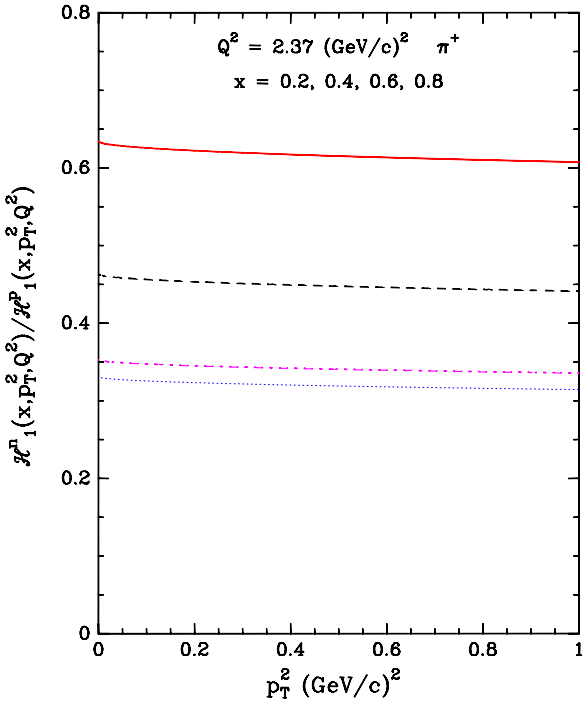

FIG. 10 (color online). The p_T^2 dependence of the ratio $\mathcal{H}_1^n/\mathcal{H}_1^p$ at $Q^2 = 2.37$ GeV^2 and $z = 0.30$ for π^+ production on a neutron and proton target. Solid line is for $x = 0.20$, dashed line for $x = 0.40$, dashed dotted line for $x = 0.60$ and dotted line for $x = 0.80$.

dependence in x and k_T. We have made some predictions for future experiments with neutron targets, which will allow further tests of our results. Major progress in our understanding of the TMD PDF will also certainly be achieved by measurements at the future electron ion collider [16].

APPENDIX

Let us consider the contribution of the diffractive term to the energy sum rule. So by using Eq. (25), this contribution reads

$$\int \frac{k_T^2}{x} q^D(x,k_T^2)dxdk_T^2 = \int_0^1 \frac{\tilde{A}x^{\tilde{b}-2}dx}{\mu^2 x^2 \ln 2(\exp\frac{x}{\tilde{x}}+1)} \times \int_0^\infty \frac{k_T^2 dk_T^2}{\exp\left(\frac{k_T^2}{x^2\mu^2}\right)+1}, \quad \text{(A1)}$$

and after the change of variable $\xi = k_T^2/x^2\mu^2$, we get

$$\mu^2 \int_0^1 \frac{\tilde{A}x^{\tilde{b}}dx}{\exp\frac{x}{\tilde{x}}+1} \int_0^\infty \frac{\xi d\xi}{\exp\xi+1} = \frac{\mu^2\pi^2 P_D}{12\ln 2}. \quad \text{(A2)}$$

One finds that $P_D = 0.0115$, so the contribution of the diffractive part to the sum rule is negligible. Finally let

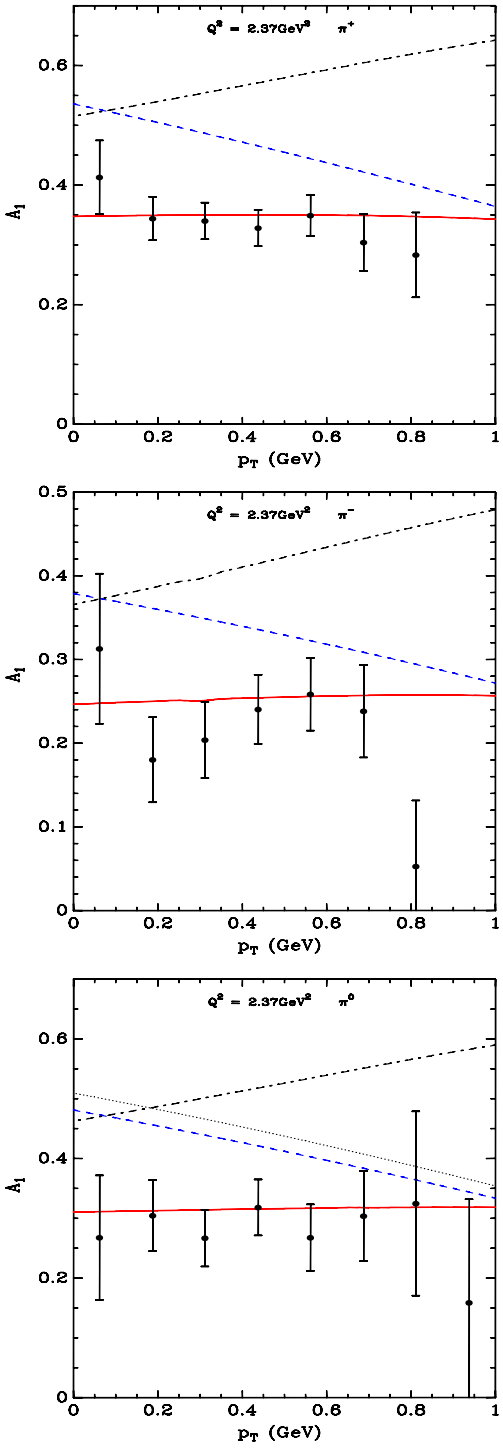

FIG. 11 (color online). The double longitudinal-spin asymmetry A_1 for π^+ (*top*), π^- (*middle*) and π^0 (*bottom*) production on a proton target, versus p_T, with the following kinematic cuts corresponding to the JLab data Ref. [15]: $0.12 < x < 0.48$, $0.4 < y < 0.85$ and $0.4 < z < 0.7$. The data displayed are those of Ref. [15] and the error bars are statistical only. The solid lines are the results from the statistical distributions and the dashed dotted lines without the inclusion of the Melosh-Wigner rotation. The dashed lines correspond to the relativistic covariant distributions and the dotted lines without the inclusion of the Melosh-Wigner rotation.

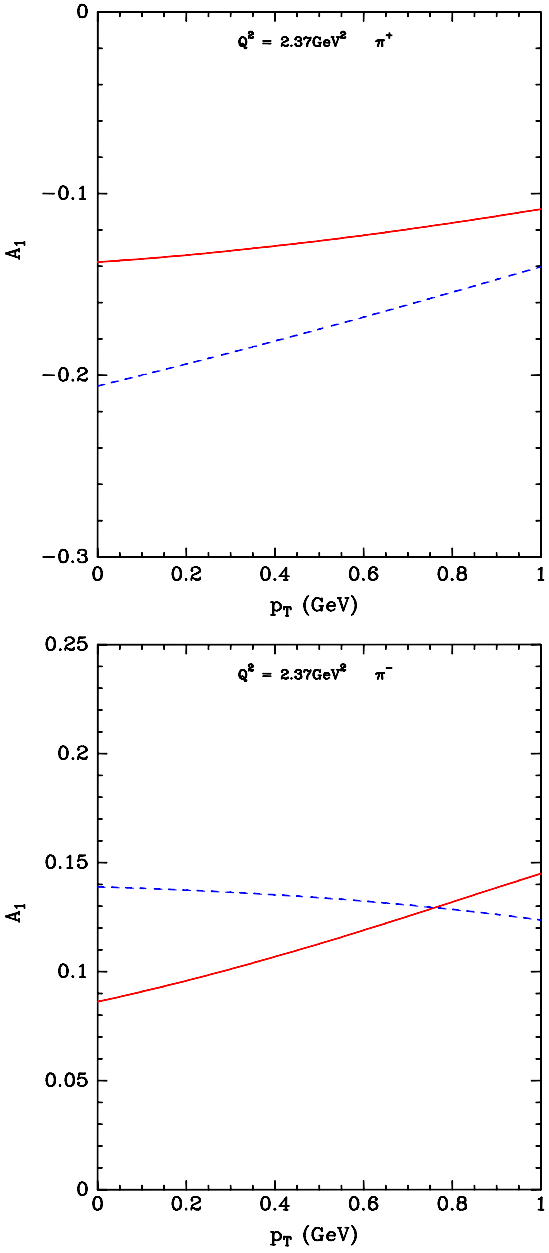

FIG. 12 (color online). The double longitudinal-spin asymmetry A_1 for π^+ (*top*), π^- (*middle*) and π^0 (*bottom*) production on a neutron target, versus p_T, assuming the same kinematic cuts as for the proton target. The solid lines are the results from the statistical distributions and the dashed lines correspond to the relativistic covariant distributions.

us consider the case of the gluon. In order to recover its x-dependence (see Eq. (5)), we can write

$$xG(x,k_T^2) = -\frac{A_G x^{b_G-2}}{(\exp\frac{x}{\bar{x}}-1)\mu^2\ln(1-\exp Y_G)} \times \frac{1}{\exp\left(\frac{k_T^2}{x^2\mu^2}+Y_G\right)-1}, \tag{A3}$$

because we had to introduce a small Y_G, otherwise $xG(x, k_T^2) = 0$. The contribution to the energy sum rule Eq. (17) is

$$\int \frac{k_T^2}{x} G(x, k_T^2) dx dk_T^2 = -\int_0^1 \frac{A_G x^{b_G - 4} dx}{\mu^2 \ln(1 - \exp Y_G)(\exp \frac{x}{\bar{x}} - 1)} \times \int_0^\infty \frac{k_T^2 dk_T^2}{\exp(\frac{k_T^2}{x^2 \mu^2} + Y_G) - 1}, \tag{A4}$$

and after the change of variable $\xi = k_T^2/x^2\mu^2$, we get

$$-\mu^2 \int_0^1 \frac{A_G x^{b_G} dx}{(\exp \frac{x}{\bar{x}} - 1) \ln(1 - \exp Y_G)} \int_0^\infty \frac{\xi d\xi}{\exp(\xi + Y_G) - 1} = \mu^2 P_G \cdot I_G, \tag{A5}$$

with

$$P_G = \int_0^1 \frac{A_G x^{b_G} dx}{\exp \frac{x}{\bar{x}} - 1} = 0.421 \tag{A6}$$

and

$$I_G = -\frac{1}{\ln(1 - \exp Y_G)} \int_0^\infty \frac{\xi d\xi}{\exp(\xi + Y_G) - 1} = -\frac{\mathrm{Li}_2(\exp Y_G)}{\ln(1 - \exp Y_G)}. \tag{A7}$$

With $Y_G = 10^{-6}$, we find $I_G = 0.119$, so the contribution of the gluon to the energy sum rule is negligible.

[1] C. Bourrely, F. Buccella, and J. Soffer, Eur. Phys. J. C **23**, 487 (2002).
[2] C. Bourrely, F. Buccella, and J. Soffer, Phys. Lett. B **648**, 39 (2007).
[3] C. Bourrely, F. Buccella, and J. Soffer, Mod. Phys. Lett. A **18**, 771 (2003).
[4] C. Bourrely, F. Buccella, and J. Soffer, Eur. Phys. J. C **41**, 327 (2005).
[5] C. Bourrely, F. Buccella, and J. Soffer, Mod. Phys. Lett. A **21**, 143 (2006).
[6] M. Anselmino *et al.*, Phys. Rev. D **74**, 074015 (2006) and references therein.
[7] H. J. Melosh, Phys. Rev. D **9**, 1095 (1974); E. Wigner, Ann. Math. **40**, 149 (1939).
[8] F. Buccella, E. Celeghini, H. Kleinert, C. A. Savoy, and E. Sorace, Nuovo Cimento A **69**, 133 (1970).
[9] P. Zavada, Eur. Phys. J. C **52**, 121 (2007) and references therein.
[10] A. V. Efremov, P. Schweitzer, O. V. Teryaev, and P. Zavada, *Proceedings of XIII Workshop on High Energy Spin Physics DSPIN-09, Dubna, Russia, September 1-5, 2009*, edited by A. V. Efremov and S. V. Goloskokov (Dubna, Dubna, Russia, 2009), p. 159; arXiv:0912.3380 and references therein; See also Proc. Sci., DIS2010 (2010) 253 [arXiv:1008.3827v1].
[11] U. D'Alesio, E. Leader, and F. Murgia, Phys. Rev. D **81**, 036010 (2010).
[12] A. Kotzinian, Nucl. Phys. **B441**, 234 (1995).
[13] S. Kretzer, Phys. Rev. D **62**, 054001 (2000).
[14] M. Osipenko *et al.* (CLAS), Phys. Rev. D **80**, 032004 (2009).
[15] H. Avakian *et al.* (CLAS), Phys. Rev. Lett. **105**, 262002 (2010).
[16] M. Anselmino, *et al.* Eur. Phys. J. A **47**, 35 (2011).